

The incidence of LBV variability in the Large Magellanic Cloud

V. M. Kalari^{1,*}, J. S. Vink², C. Furey^{2,3}, R. Salinas⁴, A. Udalski⁵, and M. Pawlak⁶

¹ Gemini Observatory/NSF's NOIRLab, Casilla 603, La Serena, Chile

² Armagh Observatory and Planetarium, College Hill, BT61 9DG Armagh, Northern Ireland, UK

³ School of Mathematics and Physics, Queen's University Belfast, Belfast BT7 1NN, UK

⁴ Nicolaus Copernicus Astronomical Center, Polish Academy of Sciences, Bartycka 18, 00-716 Warszawa, Poland

⁵ Astronomical Observatory, University of Warsaw, Al. Ujazdowskie 4, 00-478 Warszawa, Poland

⁶ Lund Observatory, Division of Astrophysics, Department of Physics, Lund University, Box 43, SE-221 00 Lund, Sweden

Received 3 October 2025 / Accepted 28 January 2026

ABSTRACT

Context. Luminous blue variables (LBVs) exhibit unique variability features, characterized by episodic outbursts (>1 mag) accompanied by spectroscopic changes (S Dor variables). The question of whether all massive stars undergo an LBV-like phase during their evolution or whether LBVs are exotic phenomena remains a matter of debate.

Aims. We aim to quantify the incidence of LBV-like variability in the blue supergiant (BSGs) population of the Large Magellanic Cloud (LMC) using the OGLE survey.

Methods. We extended the work of previous studies focused on the Small Magellanic Cloud (SMC) to the LMC, examining the light curves of 87 BSGs (out of 254 known BSGs) spanning timescales of 20 years, along with 37 objects across a three-year timescale for aperiodic variations resembling known S Dor variables.

Results. One blue supergiant, [ST92] 4-13 displays S Dor type photometric variations. Newly acquired spectra for this object reveal a potential change in spectral type, compared to the literature classification. However, based on its spectral characteristics and low luminosity and mass, we do not currently classify it as an LBV.

Conclusions. Our study highlights the need to classify bona fide LBVs as stars undergoing both photometric and spectroscopic variations. Based on currently known stellar population of S Dor variables in the LMC, the lifetime of the S Dor phase is at most $\sim 10^3$ yr. This finding is in agreement with our duty cycle study based on OGLE data in the SMC. This is several orders of magnitude shorter than what has been reported in the literature. Our discovery of LBV-like variability at low luminosities potentially suggests that S Dor variations could arise from Eddington limit-related physics over a wide range of stellar masses, rather than being linked to a unique evolutionary stage.

Key words. stars: massive – stars: variables: S Doradus – Magellanic Clouds

1. Introduction

Luminous blue variables (LBVs) are characterized by light curves with aperiodic decadal variations around 0.5–2 mag, interspersed by micro-variations on the order of 0.1–0.2 mag (also called S-Dor variables; van Genderen 2001), and (rarely) by dramatic outbursts (Conti 1997). The increase in brightness is accompanied by a color and spectral change, suggestive of an inflated envelope and a late spectral type in an eruptive phase, but an early-type supergiant when quiescent. LBVs are rather rare, with the total number of known LBVs amounting to ~ 20 across the Milky Way and Magellanic Clouds. Currently, only seven bona fide LBVs are currently known in the $1/2 Z_{\odot}$ Large Magellanic Cloud (LMC), with another four standing as candidates. Only one bona fide member, R 40, is known in the $1/5 Z_{\odot}$ Small Magellanic Cloud (SMC; Weis & Bomans 2020).

There are two potential evolutionary states characterizing LBVs. In the standard picture of massive star evolution, they would be in a transitional phase between the core hydrogen burning O star phase and the final Wolf-Rayet (WR) phase. This is oftentimes referred to as the Conti scenario (Conti 1997). In this case, the LBV duration is usually considered to be relatively short (on the order of 10^4 years) in comparison to the bulk of

the core He-burning WR phase, lasting several 10^5 years. This would be in rough agreement with the factor that there are hundreds of Wolf-Rayets in the LMC in comparison to just half a dozen LBVs.

An alternative possibility is that LBVs do not make it all the way to the WR phase, based on the notion that they might potentially be direct supernova (SN) progenitors (Kotak & Vink 2006; Smith 2007; Trundle et al. 2008). In this scenario, the LBV could either be much longer (e.g., associated with the long core He burning lifetime of 10^5 years) and only a subset of LBVs would be in a pre-SN state; alternatively, LBVs could really just be pre-SNe and very rare, with a very short lifetime of around 10^2 – 10^3 years. In the latter scenario, it has been proposed that LBV SNe could be the result of stellar merging (Justham et al. 2014; Tomblason & Smith 2015).

Alternatively, Grassitelli et al. (2021) suggested that LBV-like variations are triggered by wind-envelope interaction when stars approach the Eddington limit, as the mass loss rate increases with decreasing temperature that drives the inflation of the envelope, leading to a feedback loop corresponding to the observed variations. This model explains the observations as a physical phenomena, rather than being linked to a single evolutionary phase.

Massey et al. (2007) studied the spectral similarity of known extra-galactic LBVs to generic extragalactic supergiants, arguing

* Corresponding author: venu.kalari@noirlab.edu

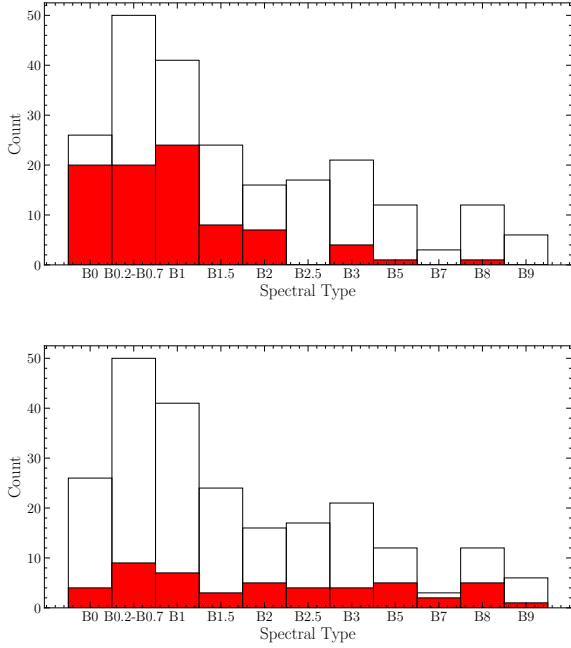


Fig. 1. *Top:* Spectral types of Bsgs with OGLE data (red) and the total number of Bsgs from our sample (solid line). *Bottom:* Recovery fraction for *Gaia* multi-epoch photometry. Known LBVs are not shown.

the LBV phenomenon could be more widespread, perhaps by as much as an order of magnitude. On the other hand, from our SMC light-curve analysis (Kalari et al. 2018), we found just one LBV candidate among the general population of B supergiants, suggesting the LBV phenomenon could be rare and special. However, a drawback of our SMC study was that we only employed three years of data, while the S Dor phase could easily last for decades (van Genderen 2001). This is the motivation behind our current study. In this paper, we expand the baseline for a similar number of objects in the LMC, but with 20 years of OGLE data, with a nearly nightly cadence allowing us to increase the temporal coverage of objects nearly sevenfold.

Our paper is organized as follows. Section 2 presents the photometric data used in this study. The analysis of light curves used in this study is described in Sect. 3. Section 4 discusses the nature of two S Dor variables identified using the analysis. Section 5 discusses the incidence of S Dor variability among BSGs, along with the light-curve analysis. Our conclusions are given in Sect. 6.

2. Data

2.1. Sample of blue supergiants

We used the Bonanos et al. (2009) catalog of massive stars in the LMC to construct our sample. Bonanos et al. (2009) compiled spectral classifications for around 1750 massive stars in the LMC based on the literature. On this basis, we identified 254 BSGs and LBVs having traceable provenance. We excluded sources with uncertain or ambiguous spectral or luminosity classifications (but we kept binaries). While our choice of input catalog misses out on potentially cool phase LBVs, our main aim is not to discover new LBVs; rather, we want to estimate the incidence of S Dor variability among known blue supergiants and, thus, this omission does not affect our results. The resulting range of spectral subtypes is shown in Fig. 1.

2.2. OGLE multi-epoch photometry

The Optical Gravitational Lensing Experiment (OGLE) survey provides high-cadence photometry in the Cousins *I* band, with observations spanning approximately June 2001 to 2020, depending on the data release. The cadence varies from a few days to weekly sampling, depending on field and observing season, and the data were obtained using the 1.3 m Warsaw telescope at Las Campanas Observatory in Chile. The median FWHM of the OGLE imaging is approximately $1''$, providing sufficient spatial resolution to resolve individual massive stars in the LMC. We refer to Udalski et al. (2015) and references therein for further details on the survey and data reduction.

We cross-matched these known BSGs with multi-epoch photometry from the OGLE-IV survey using a radius of $1''$. In cases where OGLE-IV data were unavailable, we supplemented the sample with OGLE-III data, which provide shorter temporal coverage (Udalski 2003). A total of 83 unique matches were found in the OGLE-IV dataset and 6 in the OGLE-III dataset. The OGLE dataset for each source contain typically around a thousand epochs per star, with coverage extending over nearly two decades. This enables the detection of variability phenomena on short and long timescales. The photometric precision in the *I* band is on the order of 0.01 mag for unsaturated sources and systematics are minimized through the use of difference image analysis (Wozniak 2000).

2.3. Gaia DR3 multi-epoch photometry

Gaia DR3 includes multi-epoch photometry for selected bright sources (Eyer et al. 2023). This covers observations across the custom *Gaia* *G*, *BP*, and *RP* filters spanning July 2014 to May 2017, covering between 30–80 epochs per target (except for Sk $-66^{\circ}185$, which has 175 epochs). Multi-epoch photometry was retrieved using the PYTHON astroquery package, with only photometric points satisfying the `variability_flag_g_reject` (and in the respective filters for color analysis) retained. We also ensured there were at least 25 epochs for source for the analysis. In total, there were 49 BSGs with *Gaia* DR3 multi-epoch photometry, with 11 of these also having OGLE IV light curves and 1 having an OGLE III light curve. We also retrieved the light curves of all confirmed LBVs (seven sources) from Richardson & Mehner (2018), which were not included in our input catalog from Bonanos et al. (2009). The analysis of these light curves are in Appendix A.

2.4. Recovery and completeness

Figure 1 also shows the recovery fraction of BSGs in OGLE, and *Gaia* DR3 as a function of spectral subtype. We find that approximately 36% of the BSGs identified by Bonanos et al. (2009) have light curves in the OGLE datasets. For OGLE, this is mostly because of saturation, given the saturation limit around 12 mag in *V*. This limit excludes all known LBVs in the LMC, which have apparent magnitudes brighter than ~ 12 mag in the optical (Richardson & Mehner 2018). We note that for B supergiants, on average, the magnitude stays relatively the same, or slightly increases with decreasing spectral class (for early Bs, from B0-B3 between 11–14 mag; and for latter types between 10–13 mag). A few objects fall into CCD gaps and, thus, they were not recovered. For the *Gaia* dataset, the recovery fraction is dependent on a variety of factors and is expected to increase significantly in future releases (Eyer et al. 2023).

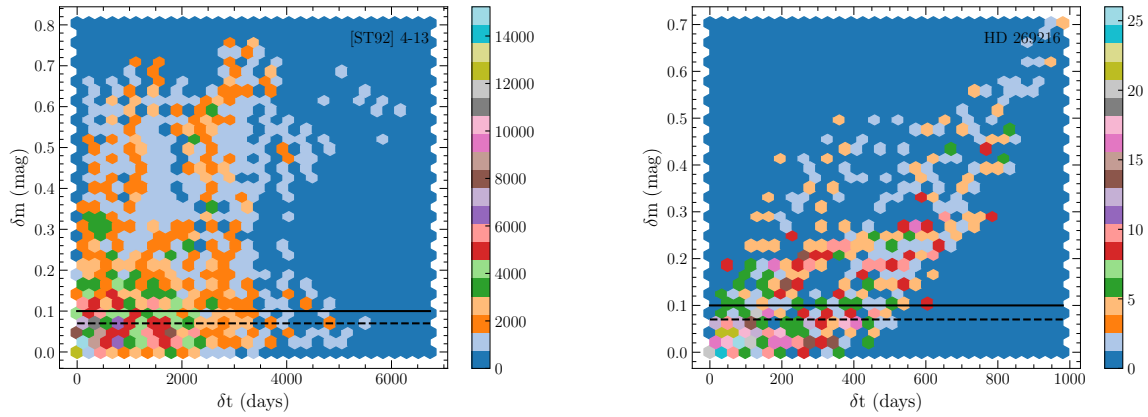


Fig. 2. Representative example of the time series photometric analysis, where the color gradient marks the density of the points. Left: LBV candidate [ST92] 4-13 $\delta m - \delta t$ histogram computed using OGLE-IV data, with the δm levels of 0.08 (10σ) and 0.1 mag marked. Right: Same as the left, but for the known LBV HD 269216, computed from *Gaia* multi-epoch photometry.

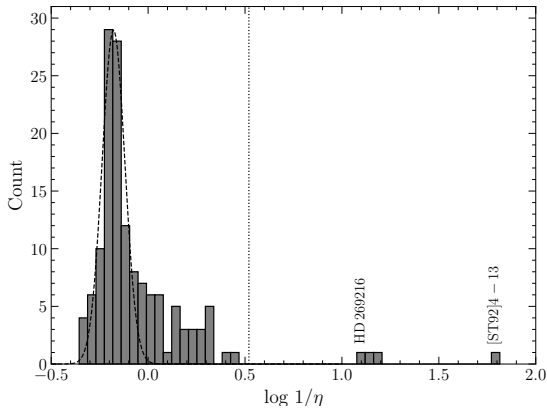


Fig. 3. Histogram of $1/\eta$ values computed using OGLE and *Gaia* light curves, in logarithmic scale. The positions of the identified LBVs, HD 269216, and [ST92] 4-13 are marked. The best-fit Gaussian to the population except the outliers ($\log(1/\eta) > 1$) is shown by the dashed line. The dotted line shows the 3σ cut-off.

The total fraction of stars with light curves is $\sim 49\%$ and this sample is biased towards earlier spectral types due to the OGLE dataset; however, a few latter spectral types are recovered from the *Gaia* photometry. For this sample size, simple binomial properties can be estimated at the 99% confidence level with a 8% margin of error given the total sample size. We note that while our selection criteria are biased due to the saturation (and faintness) limit of the photometry, considering the B spectral class as a whole, the data reflect a sufficiently representative sample for such an analysis. The list of 126 unique BSGs analyzed and their properties are electronically available via CDS, along with the complete list of 254 BSGs that are shown in Fig. 1. An representative of this is shown in Table 1.

3. Analysis of time series data

3.1. $\delta m - \delta t$ histograms

To examine aperiodic variability, we computed the $\delta m - \delta t$ plot for each light curve as described in Kalari et al. (2018), which represents the incidence of variability at a particular timescale in a light curve. It is defined as the sum of all observations at magnitude, m , and time, t , of a light curve, by computing the

differences,

$$\begin{aligned} \Delta m_{ij} &= |m_i - m_j| \quad (i > j), \\ \Delta t_{ij} &= |t_i - t_j| \quad (i > j), \end{aligned} \quad (1)$$

where $i > j$ such that each pair is only considered once. By presenting the differences between magnitude and time as a density histogram, we can directly observe how much variability is observed on what timescales. BSGs with δm greater than 0.1 mag were examined visually. The resulting $\delta m - \delta t$ plots for all sources are provided on request to the principal author. A representative example using OGLE and *Gaia* data are given in Fig. 2.

From the $\delta m - \delta t$ plots, we only identified three stars with OGLE data that show aperiodic variability above the significance threshold. The first is [ST92] 4-13 (alias W61 4-1 in SIMBAD¹, and *Gaia* DR3 4657649594536852352), a B1 I star, with the magnitude changing by nearly 1 mag over the past two decades. The other two are VFTS 698, the known binary masquerading as a B[e] star (Dunstall et al. 2012), and VFTS 652– a known spectroscopic double lined binary (Howarth et al. 2015). We discarded these two from our sample given that the magnitudes vary by less than 0.5 mag over the timescale. We only considered [ST92]4-13, as binarity is likely to be the origin of the magnitude variations in the latter two.

In the *Gaia* dataset, there is only one star with the $\delta m - \delta t$ histogram resembling a S Dor variable. HD 269216 (HIP 24347, *Gaia* DR3 4658204053297963392) is a known LBV, previously identified in Prinja & Schild (1991) and Walborn et al. (2017). Eight other stars do show aperiodic variability above 0.1 mag, but not at significant levels as those seen in [ST92]4-13 or HD 269216 (i.e. < 0.5 mag). This variability depends on a few (< 5) epochs when examining the light curves and given the scan-dependent possibility of spurious signals (Holl et al. 2023), we refrain from examining these further without future epoch photometry confirming the variability.

¹ Bonanos et al. (2009) and SIMBAD list W61 4-1 as B1 Ia based on Testor & Niemela (1998). However, this is likely to be an incorrect reference, as that paper does not include any stars from this cluster. The spectral type based on those coordinates appears to be based on the result of Schild & Testor (1992), where it is classified as star 4-13 in the cluster LH104; hence, we adopted [ST92]4-13 as the reference name. See also Skiff (2009).

Table 1. B supergiants in the LMC.

Name	Right ascension (degrees)	Declination (degrees)	Spectral type	Survey	Survey ID ¹	Simbad name	ID ²
BI 103	78.2848	-69.3011	B2 Ia	OGLE IV	LMC 503.15 93353	2MASS J05130832-6918041	388
N11-017	74.0732	-66.3051	B2.5 Iab	–	–	2MASS J04561755-6618189	99
NGC 2004-007	83.0031	-67.3396	B8 Ia	<i>Gaia</i>	DR3 4660132807190729728	CI* NGC 2004 ELS 7	964
Sk-66 185	85.6271	-66.3030	B0 Iab	OGLE IV	LMC 555.29 8272	GSC 08891-01385	1681
				<i>Gaia</i>	DR3 4659925617961629824		
Sk-68 23	75.2061	-68.1194	B3 I	OGLE III	LMC 125.2 24072	TYC 9161-1217-1	276

Notes. Coordinates are given in the J2000 epoch. The table includes objects having multi-epoch OGLE or *Gaia* photometry. Five random rows are shown, the whole table consisting of 254 objects is available at the CDS. ¹Refers to either the OGLE ID when the object has OGLE data, or *Gaia* DR3 identifier when there is *Gaia* multi-epoch photometry. ²Refers to the ID from Bonanos et al. (2009).

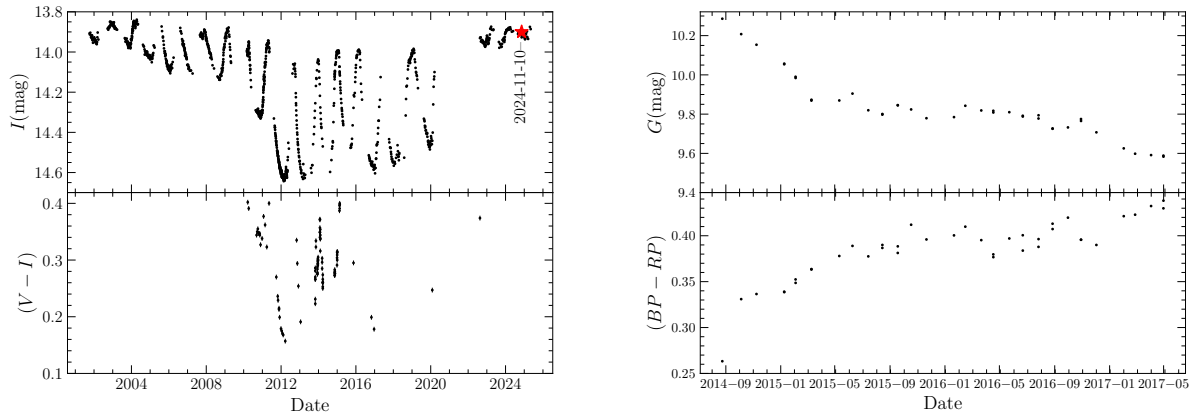


Fig. 4. *Left:* *I*-band light curve of [ST92] 4-13, with the $(V - I)$ color shown at the bottom. Data are from the OGLE-IV photometry. The red asterisk marks the epoch when the spectral data were taken. *Right:* *Gaia* *G* and $(BP - RP)$ magnitude and color light curves of HD 269216, shown at the top and bottom panel respectively.

3.2. von Neumann η index

In addition to the $\delta m - \delta t$ histograms, a method for identifying irregular variability in irregularly spaced data is via the von Neumann index (Shin et al. 2009). This index is computed as the mean squared successive difference over the variance of the distribution and acts as an indicator of independence for a series of observations (von Neumann 1941). In photometric monitoring observations, it allows us to identify whether the underlying distribution is smooth. We adopted the $1/\eta$ value, as defined in Sokolovsky et al. (2017), as a variability indicator, where larger values indicate irregular variability.

Our analysis results are shown in Fig. 3. Here, the histogram of $1/\eta$ values for our sample is shown in logarithmic scale, computed for both the *Gaia* and OGLE light curves. Three stars in the OGLE sample display values that are 3σ away from the mean of the Gaussian fitted to the distribution (peaking at $\mu = -0.15$ in log scale). These are [ST92] 4-13 with a $\log(1/\eta)$ value of 1.81, LH 104 4-67 (1.13), and LH 101 5-18 (1.18). On examining the light curve of the latter two, we find that a jump between epochs in the mean magnitude, rather than any aperiodic behavior causes these high values. In the *Gaia* dataset, HD 269216 shows a value discrepant from the median of 1.11. Overall, a comparison with the von Neumann index suggests that the same stars would have been identified for aperiodicity. The functions used to compute both the $\delta m - \delta t$ histograms and the von Neumann η index are publicly available².

² <https://github.com/astroquackers/aperiodic>

4. The S Dor variables: [ST92] 4-13 and HD 269216

4.1. [ST92] 4-13

4.1.1. Photometric variability

In Fig. 4, we show the light curve of the candidate S Dor variable—[ST92] 4-13, spanning nearly two decades. The light curve displays oscillations on the timescales of few months and the brightness decreased by 0.7 mag from 13 June 2009 to May 2012 and then increased with a larger oscillation range. In the Lomb-Scargle periodogram, we found at least four significant peaks: three of around a few days and a longer one at seven years. Large amplitude variations have ceased since 2022. Figure 4 visualizes the aperiodic change seen, showing a magnitude increase of nearly 0.8 mag seen over timescales of a year. The nearly yearly period seen along with the large amplitude variations are consistent with the changes seen for S Dor variables van Genderen (2001). For instance, van Genderen (2001) reported a period of 371.4 days for AG Car with beat cycles. *Gaia* indicators of multiplicity (RUWE and ipd_fmp) that have recovered binaries in early emission line B-type stars (Kalari et al. 2025) do not indicate that there is an unseen companion that may cause the observed light curve. Based on this information, we classified [ST92] 4-13 as a S Dor variable. We note that further unreleased OGLE observations taken between 2020-2024, which were not part of the original analysis were examined for [ST92] 4-13 and are shown in Fig. 4.

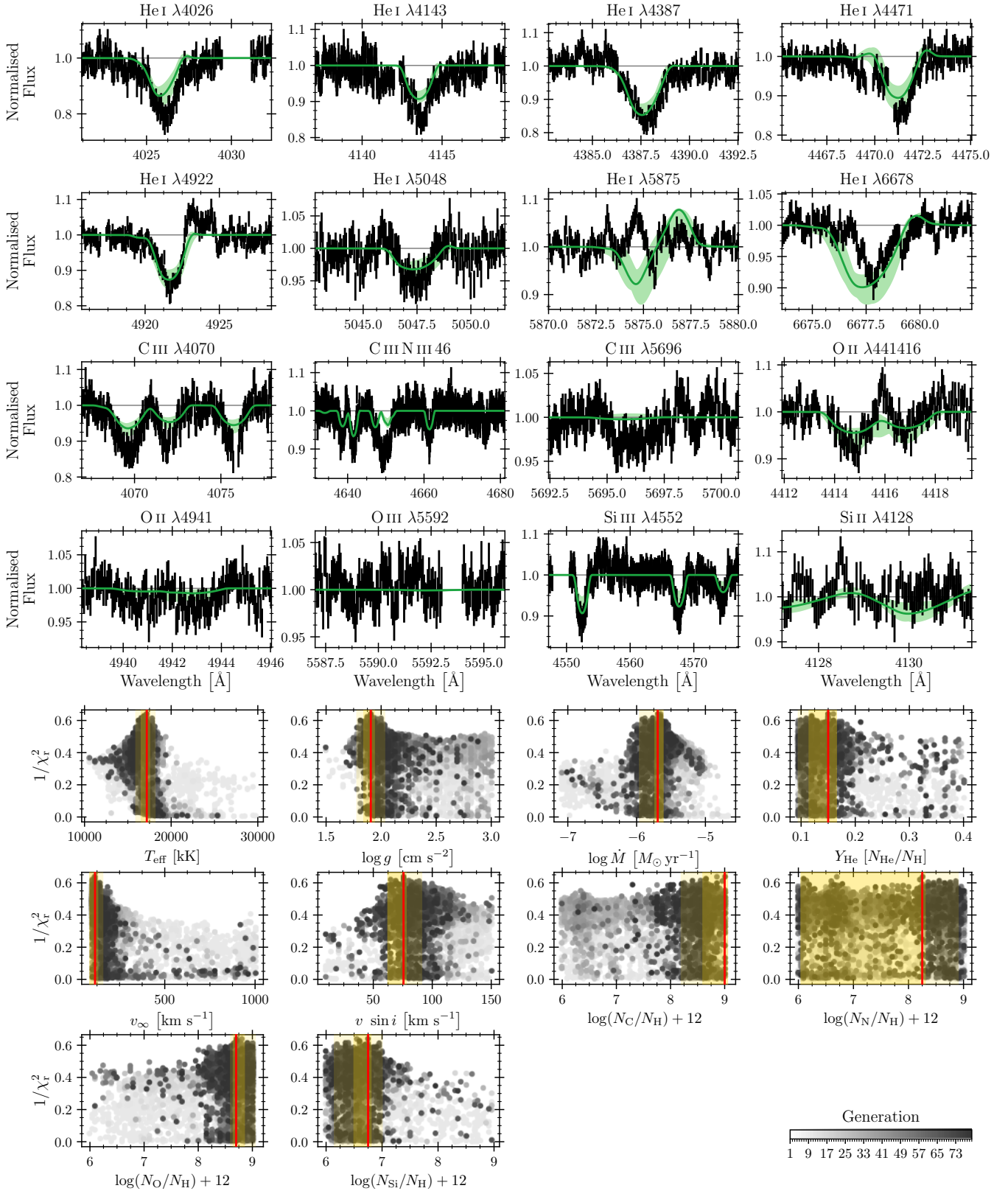


Fig. 5. KIWI-GA fit of [ST92] 4-13. See Sect. 4.1.2 for details.

4.1.2. Spectral analysis

Investigating whether there might be spectral changes accompanying the aperiodic light curve seen here, we searched the liter-

ature for spectra. [Schild & Testor \(1992\)](#) noted it as having $(B - V)$ of -0.09 and $(U - B)$ of -0.82 , with data taken between 1988 and 1990, and a spectral type of B1 Ia based on low resolution spectroscopic observations using the He I $\lambda 4471$ /Mg II $\lambda 4481$

and He I $\lambda 4144$ /He I $\lambda 4121$ line ratios within the same time frame. The object is marked as an emission line star based on the catalog of Howarth (2013); however, no line widths have been provided. *Gaia* DR3 (Gaia Collaboration 2023) XP mean spectra (reference epoch 2016.0) of the object shows a corrected H α line width of -15 \AA .

To observe whether any changes in spectral type are seen, we obtained spectra using the Gemini high-resolution optical spectrograph (GHOST) at Gemini South (Kalari et al. 2024), on November 10, 2024 (epoch marked in Fig. 4; MJD of 60624.210). Data were taken in photometric conditions with seeing around $0.8''$. Immediately after the science target, we observed the spectrophotometric standard for CPD-69 177 for absolute flux calibration. The final spectra are characterized by $R \sim 47\,000$, reaching signal-to-noise ratios (S/Ns) around 50 near the V band. The spectra display prominent Balmer emission lines, which consist of a broad and narrow emission component. The effective temperature is more representative of late-B type supergiant from the spectra, with changes observed in the H α line width compared to the Gaia spectrum (-20 \AA). The Balmer profiles do not exhibit the P Cygni morphology in the lower H lines seen in LBV candidates during quiescence (as shown in Massey et al. 2007). This is in line with the prediction that the object is heading towards visual minimum in the light curve. However, the Balmer profiles do show a P Cygni profile in He I.

To estimate the stellar parameters of [ST92] 4-13 and get an idea of its evolutionary status, we used the genetic algorithm KIWI-GA (Brands et al. 2022) in combination with the stellar atmosphere code FASTWIND (v10.6; Santolaya-Rey et al. 1997; Puls et al. 2005; Rivero González et al. 2012; Carneiro et al. 2016; Sundqvist & Puls 2018). We describe the spectral reduction process and modeling approach in Appendix B. For a more in-depth explanation of the models, we refer to the cited literature. In brief, KIWI-GA is a Python wrapper for FASTWIND that uses the concept of evolution to automatically fit FASTWIND models to an observed spectrum. Over a predefined number of generations and number of individuals per generation, the desired parameter space is explored by means of reproduction and mutation to find, for a given input spectrum, the best fitting stellar and wind parameters and statistical uncertainties. Here, we used 81 generations with 85 models per generation to estimate the stellar parameters of our target star.

The best-fitting parameters are given in Table 2, with the corresponding best-fitting spectrum and parameter posteriors shown in Fig. 5. The top four rows of the figure show the observed, continuum-normalized spectrum, and error bars in black, the best fitting FASTWIND model as the solid green line, and the 1σ uncertainty region as the shaded green region. The bottom three rows show the posteriors for each free parameter. On each of these axes, the points represent the models of the KIWI-GA run, whose colors are mapped to the generation number of the model. The red vertical line gives the best fitting value, while the dark and light yellow shaded regions give the 1- and 2σ uncertainty regions, respectively.

For [ST92] 4-13, we estimate an effective temperature $T_{\text{eff}} \simeq 17 \text{ kK}$ and surface gravity $\log(g/\text{cm s}^{-2}) \simeq 1.9$. To compute the extinction and luminosity, we drew from the VI photometry from August 19, 2022 (the closest multi-band photometry to the epoch of spectroscopic observations) of $V = 14.305$ and $I = 13.931$. We can also justify this assumption based on the fact that the I magnitude is very similar to the epoch of spectroscopic observations ($I = 13.927$ on November 10, 2024). Computing a bolometric correction in I of -1.76 and a model $(V-I)_{\text{model}}$ of -0.15 , we arrived at an A_I of 0.77 , leading to $\log(L/L_{\odot})$ of 4.73 dex.

Table 2. Best-fitting parameters and 1σ uncertainties for [ST92] 4-13 determined by KIWI-GA.

Parameter	Value
T_{eff} [kK]	$17.2^{+0.3}_{-0.6}$
$\log g$ [cm s^{-2}]	$1.9^{+0.1}_{-0.1}$
Y_{He} [$N_{\text{He}}/N_{\text{H}}$]	$0.15^{+0.02}_{-0.04}$
$v \sin i$ [km s^{-1}]	76^{+2}_{-13}
$\log \dot{M}$ [$M_{\odot} \text{ yr}^{-1}$]	$-5.7^{+0.1}_{-0.1}$
v_{∞} [km s^{-1}]	114^{+14}_{-28}
$\log(N_{\text{C}}/N_{\text{H}}) + 12$	$9.0^{+0.0}_{-0.4}$
$\log(N_{\text{N}}/N_{\text{H}}) + 12$	$8.2^{+0.1}_{-0.2}$
$\log(N_{\text{O}}/N_{\text{H}}) + 12$	$8.7^{+0.2}_{-0.0}$
$\log(N_{\text{Si}}/N_{\text{H}}) + 12$	$6.8^{+0.0}_{-0.2}$
R [R_{\odot}]	$21.8^{+0.4}_{-0.3}$

As an alternative means of computing the luminosity, we rescaled the spectral energy distribution of the best-fitting FASTWIND model to the aforementioned I magnitude, adopting a distance modulus to the LMC of 18.48 (Pietrzyński et al. 2019) and accounting for the I band extinction given above. This rescaling results in $\log(L/L_{\odot})$ of 4.57 dex. We therefore quoted an average value of the luminosity of [ST92] 4-13 as $10^{4.6 \pm 0.15} L_{\odot}$, where the uncertainties capture the discrepancies between the two methods. The object is shown on a Hertzsprung-Russell diagram, along with known LBVs from the literature in Fig. 6.

4.1.3. Classification and evolutionary status of [ST92] 4-13

The spectroscopic analysis points to change in spectral type compared to the literature, from B1a (Schild & Testor 1992) to approximately B2.5 (a change in T_{eff} of around 5 kK based on the scale of Trundle et al. 2007). However, the derived luminosity is nearly an order of magnitude lower than that of the population of known LBVs Smith et al. (2004). The star does exhibit an infrared (IR) Ca II triplet, as typically seen in LBVs, but not the forbidden [Ca II] emission or any forbidden lines seen in B[e] stars, as discussed by Humphreys et al. (2017b); it does not exhibit not the classic P Cygni profiles of LBVs in this stage either. The object is also not detected at longer wavelengths, ruling out a hot post-asymptotic giant branch (pAGB) classification (e.g. see the discussion of the potential hot pAGB/LBV star WRA 571 in Garcia-Lario et al. 1998) or even a B[e] classification (which have hot dust discs in the LMC; e.g. Kraus 2019; Kalari et al. 2014). Furthermore, there is no object currently known that would exhibit these S Dor variations other than LBVs. However, based on its low luminosity and lack of P Cygni profiles in its spectra, we consider the status of [ST92] 4-13 as a LBV to be ambiguous.

4.2. HD 269216: Photometric and spectroscopic variability

HD 269216 was first proposed as a LBV candidate on the basis of ultraviolet and optical spectra by Prinja & Schild (1991). Later, Walborn et al. (2017) compiled archival photometric and spectroscopic information detailing the outburst between 2014 and 2016, where the spectrum changed from a late-B supergiant towards an A-F type supergiant. We concur with this analysis

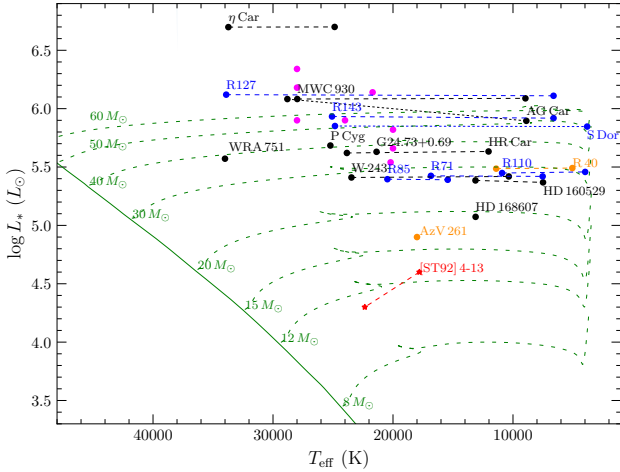


Fig. 6. Location in the HRD of [ST92] 4-13 based on Schild & Testor (1992, left), with the current observations (right) are shown in red. The positions of confirmed LBVs from the literature in the galaxy (black circles), LMC (blue circles), and the SMC (orange circle; including AzV 261, discussed in Sect. 5.1) are also shown. Magenta circles marks the position of known LBVs in M31 and M33 (from Humphreys et al. 2017a). The dashed green lines are the stellar tracks from Brott et al. (2011) with the corresponding initial stellar mass indicated, and the solid line is the zero-age main sequence isochrone for LMC metallicity.

based on the *Gaia* light curve, which has shown that the object has brightened considerably during the 2014–2016 outburst and is continuing that trend. Further monitoring of this object can track whether it has brightened since late 2020.

4.3. Circumstellar dust

Overall, LBVs show evidence of excess free-free emission (Humphreys et al. 2017b,a), similar to classical Be stars, and not containing a warm dust component as found in other LBV-like objects such as B[e] stars. In Fig. 7, we show the near-IR ($J - H$) versus ($H - K_s$) color-color diagram displaying the position of known massive stars, as well as [ST92] 4-13 and HD 269216. In addition, we also show the data in the mid-IR from WISE. In these diagrams, [ST92] 4-13 exhibits modest free-free emission at levels similar to other known S Dor LBVs. HD 269216; however, resembles most main sequence massive stars and we note that both resemble the colors of known LBVs (Humphreys et al. 2017b).

5. Discussion

5.1. S Dor variability and LBV classification

In the literature, it is common practice to refer to massive stars with major (of which are only η Car, P Cyg) or minor outbursts (for e.g. S Dor) as LBVs. The latter are often characterized as S Dor variables (after their namesake), but they are often clumped together as bona fide LBVs. LBV candidates (LBVc), on the other hand are those having spectroscopic features (e.g. deep P Cygni profiles, spectroscopic transitions between late and early supergiants, etc.), but not the accompanying photometric variations at the S Dor level.

In this paper, as well as in Kalari et al. (2018), we searched for evidence of S Dor variability among the BSG population in the LMC (and in the SMC in the earlier work). We found

evidence of one candidate in the SMC which showed S Dor type variability without any spectral changes. Here, we show another candidate [ST92] 4-13 in the LMC which demonstrates similar S Dor type variability over 20 years, but is likely not an LBV.

This brings us to the key questions of our study. For instance, we considered whether S Dor-like photometric variations unique to LBVs and where we might classify S Dor like photometric variability without the accompanying spectral variations, as in the case of the objects discussed here. Weis & Bomans (2020), Conti (1997) laid out the defining characteristic of LBVs, which is the S Dor variability or (in extremely rare cases) an η -Car like outburst. Here, we show evidence for two S Dor type variables, but with luminosity and spectral characteristics that do not resemble known LBVs.

Potential hints can be drawn from the detection of known double-lined binaries, VFTS,698 and VFTS,652 as irregular variables in our analysis, albeit with amplitudes lower than the classical S Dor variables. The former demonstrated long-term variability, but also a B[e] spectrum (and IR colors) and it was classified as W-Serpentis variable, consisting of a massive binary around a cool primary. The latter was classified as a Algol-type variable, with a low-mass primary. Compared to these two, both AzV 261 and [ST92] 4-13 are single-lined (latter a binary based on multi-epoch radial velocity variations in the He I line). It is possible that mass transfer across binary components could lead in specific cases to S Dor like light curves, such as that seen in AzV 261 (Bodensteiner et al. 2025) or [ST92] 4-13. Further high-resolution multi-epoch spectra of both these sources are necessary to understand the origin of these variations and whether they can be attributed to binary mass transfer or if they are accompanied by spectral type changes. It might also be the case that most LBVs are born from mergers of hierarchical triple systems (Hirai et al. 2021) and the two stars discussed here could be the lower mass counterparts of such interactions. With the advent of multi-epoch photometry from surveys such as LSST, care must be taken in defining the variability of LBVs based on photometric variability. In this case, LBV should only be classified as such when observed with accompanying spectral characteristics. Drawing from the duck analogy laid out in Conti (1997) and Massey et al. (2007), we suggest that if an LBV shows photometric and spectroscopic variability, it should be classified as an LBV; and if only shows one or the other, it should be classified as a LBVc.

An alternative explanation for [ST92] 4-13 and AzV 261 could be that these objects are the observational indication of low-luminosity LBVs (Smith et al. 2004). It has been proposed using rotating evolutionary models (Levesque et al. 2025; Meynet & Maeder 2005) that stellar rotation lowers the mass (and thereby luminosity) threshold of the LBV phase. At solar metallicities, this is predicted to be around $22 M_{\odot}$, although the mass limit is thought to increase at lower metallicities and to be dependent on the rotational velocity.

At LMC metallicity, for an initial velocity of 300 km s^{-1} , Meynet & Maeder (2005) found a lower initial mass limit of $25 M_{\odot}$. The initial mass of [ST92] 4-13 is lower than this limit; hence, we considered this possibility to be unlikely. Instead, we considered that the examples of the S Dor type phenomena at even lower luminosities (and by inference lower masses) reported here and in Kalari et al. (2018) might not actually be linked to a single evolutionary phase; rather, they could be caused by Eddington-limit related physics at a range of masses, which could involve certain processes such as binary evolution.

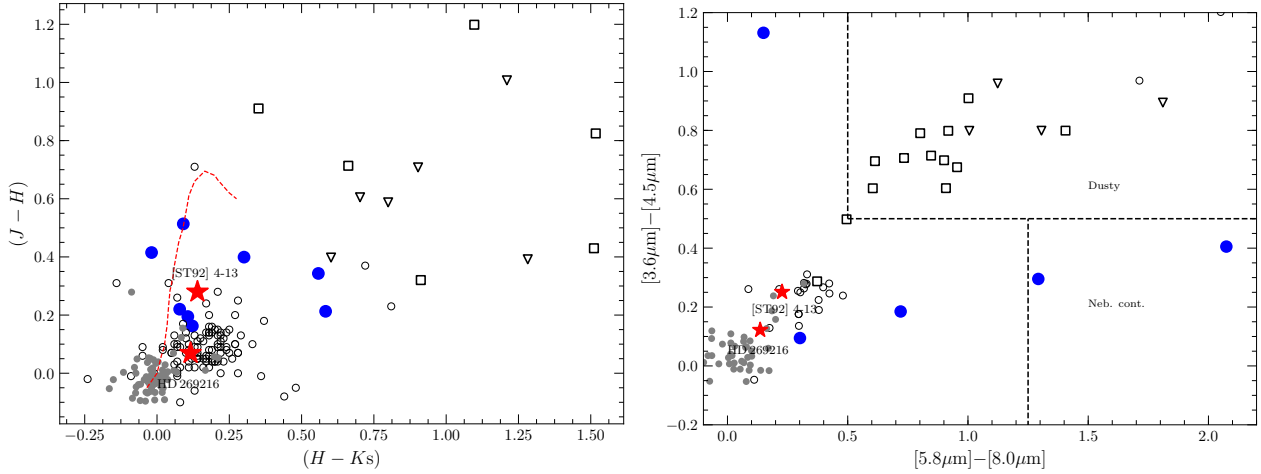


Fig. 7. *Left:* Near-IR $(J-H)$ vs. $(H-K_s)$ color-color diagram of known sgB[e] (open squares), warm hypergiants (open triangles), cBe stars (open circles), known S Dor variables (blue dots), BSGs (small dots), and [ST92] 4-13, HD 269216 (red asterisks). Data taken from Humphreys et al. (2017b). The dashed red line is the main-sequence locus. *Right:* Mid-IR $[3.6\ \mu\text{m}]-[4.5\ \mu\text{m}]$ vs. $[5.8\ \mu\text{m}]-[8.0\ \mu\text{m}]$ color-color diagram.

5.2. S Dor variables among the Bsg population

The primary motivation of our study was to follow up on our previous results presented Kalari et al. (2018), but with a longer baseline and to cover a large sample size by studying BSGs in the LMC. In that study, based in the SMC, over a three-year baseline observation of 64 BSGs, we detected only one potential S Dor variable (AzV 261), which did not show any spectral type variation. Here, covering a sample size of 87 (37) across a 20 (3) year timescale, we found two objects exhibiting S Dor-type variations. One was the known LBV, HD 269216 and the other was the newly identified S Dor variable [ST92] 4-13. The latter exhibits a potential change in spectral type from B1 (literature) to B2.5, but its luminosity is too low to be classified as an LBV. In addition, its spectra do not show the P Cygni profiles caused due to strong mass loss of LBVs.

Under the assumption that all known LBVs have been discovered from the Bsgs population of the LMC galaxy (8, and 4 candidate S Dor variables from 250 known Bsgs according to census compiled by Bonanos et al. 2009), we estimate the duty cycle of the S Dor phase to be at most \sim few 10^3 yr (assuming a He-burning lifetime of 10^5 years). This is similar to the value found for the SMC (Kalari et al. 2018).

The prior work carried out on the SMC was based on multi-epoch photometry covering a three-year baseline. In the present study, we expanded the baseline and sample size. The similarity of the duty cycle estimated by the two studies at different metallicity values suggest that, based on the current observational limitations in magnitude range and baselines, the S Dor duty cycle is at least an order of magnitude shorter than commonly assumed. Moreover, BSGs and LBVs are truly different evolutionary stages in the life-cycle of massive stars. In other words, we find that BSGs are not dormant LBVs.

6. Conclusions

Here, we have improved on previous searches for LBV variability among BSGs by increasing the baseline and sample size from the previous work of Kalari et al. (2018). We examined the 20-year nearly nightly cadence light curves of 87 BSGs from OGLE, along with the 3-year *Gaia* multi-epoch photometry of 37 BSGs in the LMC. As a result, we found evidence for S Dor-

type variability found in LBVs for one known LBV (HD 269216) and one BSG ([ST92] 4-13). Our conclusions are listed below.

- Despite an increased sample size and baseline, the duty cycle we found for LBVs was roughly similar at around 10^3 years. This suggests that LBVs are truly unique or transitory objects and it is unlikely for the LBV phenomenon to be widespread among the general BSG population.
- We also argue that both photometric and spectral type variations, along with spectral characteristics and high-luminosities are necessary to classify LBVs, based on the properties of the candidates presented here.
- Our findings suggest that LBV-like variability is a physical phenomena and not and not solely linked to any one particular evolutionary phase.

Our study in the LMC agrees with previous findings in the SMC that the duty cycle of LBVs is around 10^3 years, and that LBVs appear to be unique, transitory objects rather than dormant BSGs. The discovery of LBV-like photometric variability in stars that do not show other LBV characteristics suggests that the variability is a physical phenomenon rather than an evolutionary one.

Data availability

The full Table 1 is available at the CDS via <https://cdsarc.cds.unistra.fr/viz-bin/cat/J/A+A/708/A343>

Acknowledgements. V. M.K. is supported by the international Gemini Observatory, a program of NSF NOIRLab, which is managed by the Association of Universities for Research in Astronomy (AURA) under a cooperative agreement with the U.S. National Science Foundation, on behalf of the Gemini partnership of Argentina, Brazil, Canada, Chile, the Republic of Korea, and the United States of America. The OGLE project has received funding from the Polish National Science Centre grant OPUS-28 2024/55/B/ST9/00447 to AU. This work presents results from the European Space Agency (ESA) space mission *Gaia*. *Gaia* data are being processed by the *Gaia* Data Processing and Analysis Consortium (DPAC). Funding for the DPAC is provided by national institutions, in particular the institutions participating in the *Gaia* MultiLateral Agreement (MLA). The *Gaia* mission website is <https://www.cosmos.esa.int/gaia>. The *Gaia* archive website is <https://archives.esac.esa.int/gaia>. This research has made use of the SIMBAD database, CDS, Strasbourg Astronomical Observatory, France.

References

- Bodensteiner, J., Shenar, T., Sana, H., et al. 2025, *A&A*, 698, A38
- Bonanos, A. Z., Massa, D. L., Sewilo, M., et al. 2009, *AJ*, 138, 1003
- Brands, S. A., de Koter, A., Bestenlehner, J. M., et al. 2022, *A&A*, 663, A36
- Brott, I., de Mink, S. E., Cantiello, M., et al. 2011, *A&A*, 530, A115
- Carneiro, L. P., Puls, J., Sundqvist, J., & Hoffmann, T. 2016, *A&A*, 590, A88
- Conti, P. S. 1997, in *Luminous Blue Variables: Massive Stars in Transition*, eds. A. Nota, & H. Lamers, *ASP Conf. Ser.*, 120, 387
- Dunstall, P. R., Fraser, M., Clark, J. S., et al. 2012, *A&A*, 542, A50
- Eyer, L., Audard, M., Holl, B., et al. 2023, *A&A*, 674, A13
- Gaia Collaboration (Vallenari, A., et al.) 2023, *A&A*, 674, A1
- García-Lario, P., Riera, A., & Machado, A. 1998, *A&A*, 334, 1007
- Grassitelli, L., Langer, N., Mackey, J., et al. 2021, *A&A*, 647, A99
- Hirai, R., Podsiadlowski, P., Owocki, S. P., Schneider, F. R. N., & Smith, N. 2021, *MNRAS*, 503, 4276
- Holl, B., Fabricius, C., Portell, J., et al. 2023, *A&A*, 674, A25
- Howarth, I. D. 2013, *A&A*, 555, A141
- Howarth, I. D., Dufton, P. L., Dunstall, P. R., et al. 2015, *A&A*, 582, A73
- Humphreys, R. M., Davidson, K., Hahn, D., Martin, J. C., & Weis, K. 2017a, *ApJ*, 844, 40
- Humphreys, R. M., Gordon, M. S., Martin, J. C., Weis, K., & Hahn, D. 2017b, *ApJ*, 836, 64
- Justham, S., Podsiadlowski, P., & Vink, J. S. 2014, *ApJ*, 796, 121
- Kalari, V. M., Vink, J. S., Dufton, P. L., et al. 2014, *A&A*, 564, L7
- Kalari, V. M., Vink, J. S., Dufton, P. L., & Fraser, M. 2018, *A&A*, 618, A17
- Kalari, V. M., Diaz, R. J., Robertson, G., et al. 2024, *AJ*, 168, 208
- Kalari, V. M., Salinas, R., Saez-Carvajal, C., et al. 2025, *ApJ*, 993, 192
- Kotak, R., & Vink, J. S. 2006, *A&A*, 460, L5
- Kraus, M. 2019, *Galaxies*, 7, 83
- Levesque, E. M., Lamers, H. J. G. L. M., & de Koter, A. 2025, *ApJ*, 981, 176
- Massey, P., McNeill, R. T., Olsen, K. A. G., et al. 2007, *AJ*, 134, 2474
- McErlean, N. D., Lennon, D. J., & Dufton, P. L. 1999, *A&A*, 349, 553
- Meynet, G., & Maeder, A. 2005, *A&A*, 429, 581
- Pietrzyński, G., Graczyk, D., Gallenne, A., et al. 2019, *Nature*, 567, 200
- Prinja, R. K., & Schild, H. 1991, *A&A*, 249, 428
- Puls, J., Urbaneja, M., Venero, R., et al. 2005, *A&A*, 435, 669
- Richardson, N. D., & Mehner, A. 2018, *Res. Notes Am. Astron. Soc.*, 2, 121
- Rivero González, J., Puls, J., Najarro, F., & Brott, I. 2012, *A&A*, 537, A79
- Santolaya-Rey, A. E., Puls, J., & Herrero, A. 1997, *A&A*, 323, 488
- Schild, H., & Testor, G. 1992, *A&AS*, 92, 729
- Shin, M.-S., Sekora, M., & Byun, Y.-I. 2009, *MNRAS*, 400, 1897
- Skiff, B. A. 2009, *CDS/ADC Collection of Electronic Catalogues*, 1, 2023 (2009)
- Smith, N. 2007, in *Supernova 1987A: 20 Years After: Supernovae and Gamma-Ray Bursters*, eds. S. Immler, K. Weiler, & R. McCray, *AIP Conf. Ser.*, 937, 163
- Smith, N., Vink, J. S., & de Koter, A. 2004, *ApJ*, 615, 475
- Sokolovsky, K. V., Gavras, P., Karamelas, A., et al. 2017, *MNRAS*, 464, 274
- Sundqvist, J., & Puls, J. 2018, *A&A*, 619, A59
- Testor, G., & Niemela, V. 1998, *A&AS*, 130, 527
- Tombleson, R., & Smith, N. 2015, *Am. Astron. Soc. Meeting Abstr.*, 225, 343.17
- Trundle, C., Dufton, P. L., Hunter, I., et al. 2007, *A&A*, 471, 625
- Trundle, C., Kotak, R., Vink, J. S., & Meikle, W. P. S. 2008, *A&A*, 483, L47
- Udalski, A. 2003, *Acta Astron.*, 53, 291
- Udalski, A., Szymański, M. K., & Szymański, G. 2015, *Acta Astron.*, 65, 1
- van Genderen, A. M. 2001, *A&A*, 366, 508
- van Genderen, A. M., & Sterken, C. 1999, *A&A*, 349, 537
- von Neumann, J. 1941, *Ann. Math. Stat.*, 12, 367
- Walborn, N. R., Gamen, R. C., Morrell, N. I., et al. 2017, *AJ*, 154, 15
- Weis, K., & Bomans, D. J. 2020, *Galaxies*, 8, 20
- Wozniak, P. R. 2000, *Acta Astron.*, 50, 421

Appendix A: $\delta m - \delta t$ histograms and η index of confirmed LMC LBVs

We retrieved *Gaia* DR3 multi-epoch photometry of confirmed LBVs listed in Richardson & Mehner (2018, see Sect. 2.3). There are seven sources, all of which had multi-epoch photometry spanning the DR3 period (3 years). We show in Fig. A.1 the histograms computed as described in Sect. 3.1, utilizing the *G*-band photometry. Only data points with `variability_flag_g_reject=False` were used in any analysis. The histograms all have aperiodic variability above the significance level. The distribution of the histograms are similar to the LBV HD 269216 and [ST92] 4-13, but the histogram of [ST92] 4-13 also shows a periodic trend along with aperiodic variability (both vertical and inclined lines).

In the top-right of each histogram, the $1/\eta$ index is given, and computed as described in Sect. 3.2. All stars have significant indexes except for HD 269700, representative of aperiodic variability. The lack of variability is not surprising for HD 269700, since it is considered an ex/dormant LBV (van Genderen & Sterken 1999). All these stars would be selected as an LBV with our analysis methodology, indicating our method is suitable to recover LBVs. Future multi-epoch photometry from *Gaia*³ covering a much larger baseline can be used to search for further possible LBVs in the Magellanic Clouds.

Appendix B: Modeling approach for [ST92] 4-13

In this section, we describe how we prepared the optical spectrum of [ST92] 4-13 to be analyzed. First, we decided on a list of diagnostic spectral lines. With the main goal of this exercise being to gauge the evolutionary status of our target, we are primarily interested in the determination of the effective temperature (T_{eff}) and surface gravity (g) from its spectrum, along with the luminosity (L) from these. For T_{eff} , we used the Si II to Si III ratio; the primary temperature diagnostic in B stars (e.g. McErlean et al. 1999). We used the photospheric He I lines to constrain g . As these lines show wind features, we also use them to get an idea of the mass loss rate (\dot{M}) and terminal wind speed (v_{∞}). Regarding the wind structure, we assumed a fixed clumping factor of 10 and that all clumps in the wind are optically thin. We also estimate the projected rotational velocity, $v \sin i$. We do not account for macroturbulent broadening here, so our quoted value of 76_{-13}^{+2} km s⁻¹ in Table 2 is an upper limit of the true projected rotational velocity. Finally, we left the helium abundance ($Y_{\text{He}} := N_{\text{He}}/N_{\text{H}}$), and C, N, O, and Si abundances as free parameters in our fit.

While the spectrum of our target exhibits strong Balmer emission, indicative of a dense stellar wind, we do not fit these lines here. Our current assumptions regarding the wind structure are not enough to adequately describe the nature of the stellar wind; simultaneous modelling of the UV spectrum, where resonance lines of metals lie, would be needed to gain a complete picture of the wind of this star. From a test run where the Balmer lines were included, we found they strongly biased T_{eff} and g to very high values to compensate for our assumptions regarding the wind structure, resulting in an overall very poor fit. In any case, we are not interested in studying \dot{M} here, so we left them out for these reasons.

FASTWIND and KIWI-GA requires a radial velocity-corrected, continuum-normalised spectrum as input. To correct for the radial velocity, we performed a cross-correlation using

a template of Gaussian absorption profiles at the wavelengths of the photospheric He I profiles, as well as at the three components of the Si III $\lambda 4452$ profile. From this we find a radial velocity of 269 ± 38 km s⁻¹.

Once corrected for radial velocity, we locally normalised the target spectral lines. For a given line, this involved masking spectral features blue and red of the line, fitting a line through the local continuum level, and dividing through by this line. This is a reasonable approach given the relatively few spectral lines in the optical spectrum. In some instances, it was necessary to fit degree 2 polynomials to the continuum. This was the case for C III $\lambda 4070$, He I $\lambda 4143$, and the O II doublet at 4416 Å.

³ <https://www.cosmos.esa.int/web/gaia/dr4#>

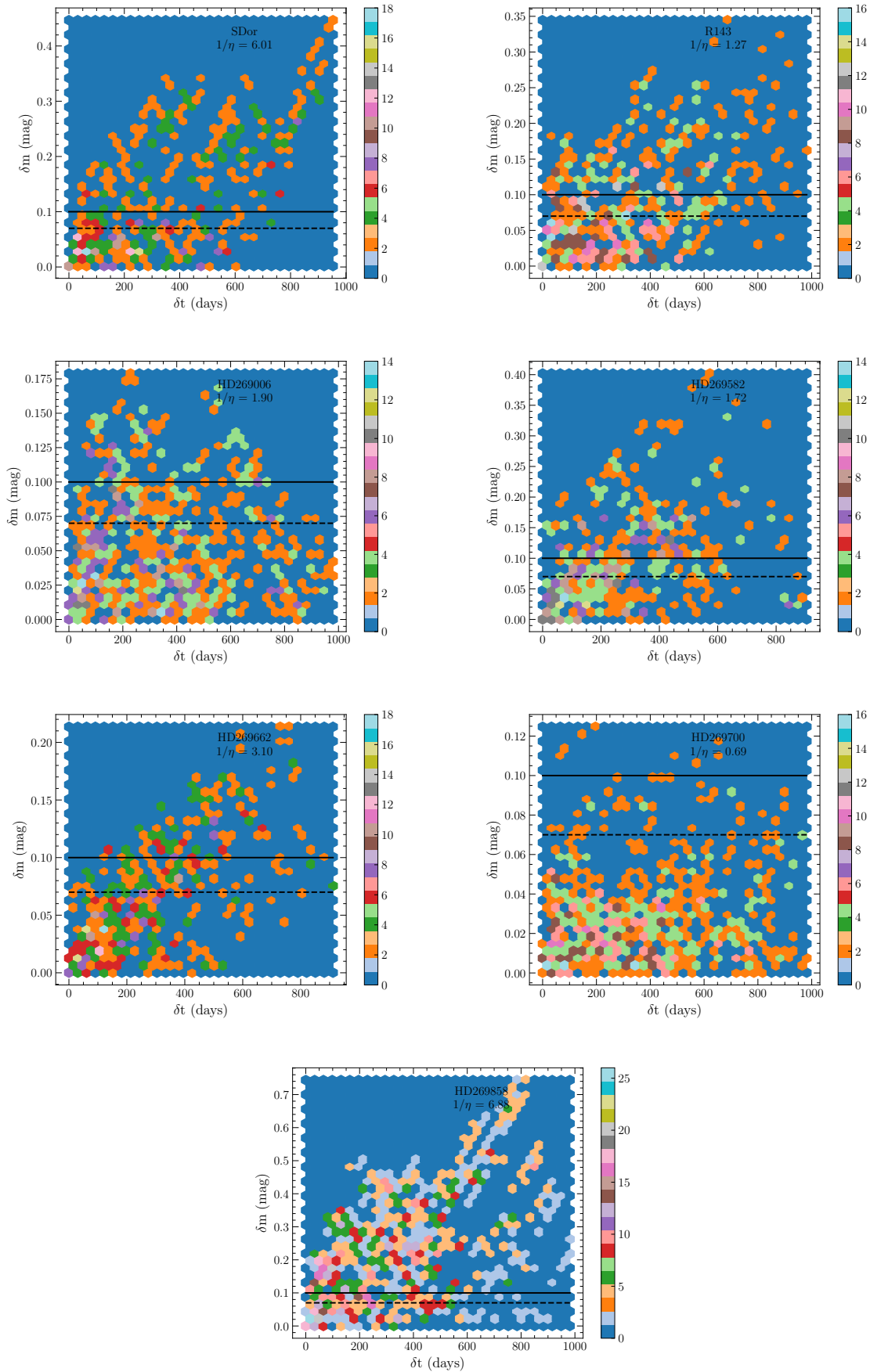


Fig. A.1. $\delta m - \delta t$ histograms of confirmed LMC LBVs, with the $1/\eta$ value given in the top right.